

Shapes of Hyperspectral Imaged Microplastics

Liu, Fan; Rasmussen, Lasse Abraham; Klemmensen, Nanna Dyg Rathje; Zhao, Guohan; Vianello, Alvise; Rist, Sinja ; Vollertsen, Jes

Published in:
Environmental Science & Technology

DOI (link to publication from Publisher):
[10.1021/acs.est.3c03517](https://doi.org/10.1021/acs.est.3c03517)

Creative Commons License
CC BY-NC-ND 4.0

Publication date:
2023

Document Version
Publisher's PDF, also known as Version of record

[Link to publication from Aalborg University](#)

Citation for published version (APA):
Liu, F., Rasmussen, L. A., Klemmensen, N. D. R., Zhao, G., Vianello, A., Rist, S., & Vollertsen, J. (2023). Shapes of Hyperspectral Imaged Microplastics. *Environmental Science & Technology*, 57(33), 12431-12441. <https://doi.org/10.1021/acs.est.3c03517>

General rights

Copyright and moral rights for the publications made accessible in the public portal are retained by the authors and/or other copyright owners and it is a condition of accessing publications that users recognise and abide by the legal requirements associated with these rights.

- Users may download and print one copy of any publication from the public portal for the purpose of private study or research.
- You may not further distribute the material or use it for any profit-making activity or commercial gain
- You may freely distribute the URL identifying the publication in the public portal -

Take down policy

If you believe that this document breaches copyright please contact us at vbn@aub.aau.dk providing details, and we will remove access to the work immediately and investigate your claim.

Shapes of Hyperspectral Imaged Microplastics

Fan Liu,* Lasse A. Rasmussen, Nanna D. R. Klemmensen, Guohan Zhao, Rasmus Nielsen, Alvise Vianello, Sinja Rist, and Jes Vollertsen



Cite This: *Environ. Sci. Technol.* 2023, 57, 12431–12441



Read Online

ACCESS |



Metrics & More



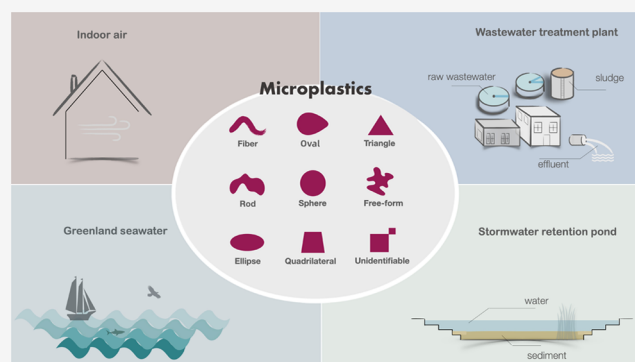
Article Recommendations



Supporting Information

ABSTRACT: Shape matters for microplastics, but its definition, particularly for hyperspectral imaged microplastics, remains ambiguous and inexplicit, leading to incomparability across data. Hyperspectral imaging is a common approach for quantification, yet no unambiguous microplastic shape classification exists. We conducted an expert-based survey and proposed a set of clear and concise shapes (*fiber, rod, ellipse, oval, sphere, quadrilateral, triangle, free-form, and unidentifiable*). The categories were validated on images of 11,042 microplastics from four environmental compartments (seven matrices: indoor air; wastewater influent, effluent, and sludge; marine water; stormwater; and stormwater pond sediments), by inviting five experts to score each shape. We found that the proposed shapes were well defined, representative, and distinguishable to the human eye, especially for *fiber* and *sphere*. *Ellipse, oval, and rod* were though less distinguishable but dominated in all water and solid matrices. Indoor air held more *unidentifiable*, an abstract shape that appeared mostly for particles below 30 μm . This study highlights the need for assessing the recognizability of chosen shape categories prior to reporting data. Shapes with a clear and stringent definition would increase comparability and reproducibility across data and promote harmonization in microplastic research.

KEYWORDS: shape, microplastic, hyperspectral image, pixelization, manual classification, ground truth



1. INTRODUCTION

Microplastic is an emerging pollutant that potentially poses risks to humans and the environment, and its occurrence has been documented virtually everywhere.^{1–4} The impact of microplastics on organisms is associated with their shape, additives, and sorbed chemicals. For instance, spherical polystyrene (PS) beads exhibited higher toxicity than irregular fragments and fibers on *Daphnia magna*.⁵ Particle shape also matters for physical behavior like settling velocities.^{6,7} It was found that a shape-dependent approach outperformed in predicting terminal settling velocities compared to simply assuming all particles were spheres,⁸ and the aerodynamics of microplastics depends highly on shape.⁹ Biochemically, shape can affect the biofouling of microplastics and hereby their environmental fate,^{10,11} as well as the adsorbed and leached chemicals.^{12,13}

Much microplastic identification has been done by visual inspection,¹⁴ with *foam, flake, film, and sponge* often used shape classes. These categories require knowledge on the particle's third dimension,¹⁵ which is achievable for larger particles, but increasingly uncertain as size decreases. Visual-based classification furthermore has its limitations as not all particles that resemble microplastics are of synthetic origin. Hyperspectral imaging has proven its worth in this respect with accurate quantification of chemical composition, especially when it

comes to small microplastics, which also are more abundant than the larger ones.^{16–18}

Hyperspectral imaging creates a 2-dimensional projection of a particle.¹⁹ Shapes requiring a third dimension, e.g., *film, flake, and sponge*, hence cannot be used as classes for the so-imaged microplastics. A suitable shape category should, furthermore, be unambiguous and precise in describing a particle's geometry. Commonly used shapes such as *fiber, fragment, flake, pellet, bead, and foam* are illustrative but not always well defined.^{20,21} Still, many studies apply shape classes without clear geometric definitions, for instance, what characteristics define a *fragment* or a *foam*?^{5,22} Even with a clear definition, some shapes are only suitable for visual identification but not hyperspectral imaged microplastics, for instance, *film*.²⁰ While unambiguous and precise geometric shapes can readily be defined, e.g., *sphere, rectangle, and oval*, it can be difficult to assign them to real microplastics as these can be of any shape.

Received: May 10, 2023




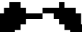








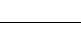
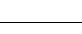




Revised: July 25, 2023

Accepted: July 26, 2023

Published: August 10, 2023



Table 1. Applied Reference Shapes with Idealized Forms, Examples of Pixelized Images of Environmental Microplastics, and Examples of Where the Shapes Have Been Applied

Category	Idealized form	Actual microplastic	Form	Angularity	Description and application in other fields	Shape merging
<i>Fiber</i>			Elongated	Rounded	Elongated form, rounded, the diameter is constant along the longest path of its skeleton. Examples of applications: sediments, soils, dust, ⁴¹ minerals, ⁴² microplastics. ⁴³	Can be merged with <i>rod</i> if the degree of diameter fluctuation along the skeleton is not of interest.
<i>Rod</i>					Elongated form, rounded, the diameter fluctuates along its skeleton. Examples of applications: bacterial cells, ⁴⁴ microplastics, ⁴⁵ sediment, ⁴⁶ wollastonite. ⁴⁷	Can be merged with <i>fiber</i> if the degree of diameter fluctuation along the skeleton is not of interest.
<i>Ellipse</i>			Less elongated		Less elongated form, rounded, symmetric in both axes. Examples of applications: aggregates, ⁴⁸ sediments, ⁴⁹ microplastics, ¹⁶ nanoparticles. ⁵⁰	Can be merged with <i>oval</i> if the number of symmetric axes is not of interest.
<i>Oval</i>					Less elongated form, rounded, symmetric in one axe. Examples of application: microplastics. ^{45,51}	Can be merged with <i>ellipse</i> if the number of symmetric axes is not of interest. Or be merged with <i>sphere</i> if particle form is not of research interest.
<i>Sphere</i>			Not elongated		Angular	Circular in form, rounded. Examples of applications: minerals, ⁵² microplastics. ⁵³
<i>Quadrilateral</i>				Not elongated in form, angular, has four distinguishable angles. Examples of application: microplastics. ⁵³		Can be merged with <i>sphere</i> if angularity is not of interest.
<i>Triangle</i>					Not elongated in form, angular, has three distinguishable angles. Examples of application: microplastics. ⁵⁴	Can be merged with <i>oval</i> if angularity and particle form are not of interest.
<i>Free-form</i>					Unevenly distributed curves and angular contours, or a combination of both. Examples of application: particle transport, ⁵⁵ traffic obstacles, ⁵⁶ bitten objects, ⁵⁷ optical elements. ⁵⁸	Not recommended merged with other shapes.
<i>Unidentifiable</i>					An abstract shape which cannot be identified due to a limited pixel number. Examples of application: Scene recognition, ⁵⁹ microplastics. ⁶⁰	Not recommended merged with other shapes.

Furthermore, the number of potential categories is legion, leading to the question: Which shapes to choose?

2D imaging has a long history when classifying soil²³ and minerals.^{24,25} Two approaches are traditionally used:^{26,27} (a) assigning a shape by manually comparing the particle to a reference shape chart and (b) measuring geometric parameters (e.g., circularity) and applying them to decide on a shape. However, actual shapes often fall between reference shapes; thus, choosing a single shape tends to be insufficient. Applying measured geometric parameters has the benefit of removing observer bias, but converting these into usable shape categories is not trivial. Models must be trained with a data set defining “ground truth”, which again relies on specialists assigning shapes to particles. In both cases, what comes first is choosing reasonable reference shapes, after which real particles must be categorized by specialists. This can then either be used directly or be used to train a mathematical model.

Our study attempts to define a set of geometrically well-defined and representative shape categories, which are suited for imaged microplastics. To validate the shapes and examine their application, we invited experts to manually evaluate the 2D images of 11,042 environmental microplastics. The

obtained data set is further used to analyze the distinguishability, divergence, and confusion in perceiving the proposed shapes, as well as the shape distribution of microplastics in distinct environmental matrices.

2. METHODOLOGY

2.1. Microplastics from Environmental Samples.

Microplastics from four environmental compartments, including seven matrices, were chosen, together supplying 11,042 hyperspectral images for shape analysis. They comprised marine water,²⁸ wastewater treatment plant (WWTP) influent and effluent,²⁹ stormwater,¹⁷ WWTP sludge,³⁰ stormwater pond sediments,³¹ and indoor air samples.³² The lower size limit for all studies was 11 μm , and all images were acquired by the same instrument, an FPA- μFTIR imaging spectroscope (Focal Plane Array-based Fourier Transform Infrared Spectroscopy, Agilent) at a pixel resolution of 5.5 μm . The acquired hyperspectral maps were analyzed with the freeware siMPle for MP detection and quantification.³³ siMPle produces a pixelated hyperspectral image of each particle and gives its polymer type and size. The latter is defined as the longest

linear distance between pixels corresponding to a particle. Examples of acquired images are shown in Table 1.

2.2. Shape Categories of Microplastics. The question of which shape categories are often seen and representative must be answered before the manual shape assignment can be processed. Here, we employed a focus group discussion, which has been widely applied in sociology, psychology, and marketing.³⁴ We assembled a group of experts to discuss a specific topic and draw a conclusion from it, an approach that is perceived as a cost-effective and semiquantitative method in participatory research.³⁵ Yet, the choice of what are relevant shapes can be driven by personal experiences, and cognitive perception hence becomes subjective. To minimize the subjectivity, we invited five experts who work with imaged microplastics to discuss the following questions:

- What are the often-seen shapes according to your own research experiences?
- Which geometries do you deem representative of these shapes and should be included as reference shapes?

The answers pointed toward the shapes *fiber*, *ellipse*, and *sphere* being common, while several other shapes occurred at lower frequencies.

The selected reference shapes should preferably cover as much geometric variability as possible without leading to too many categories. When manually assessing a large data set (11,042 particles), too many categories would result in a “choice overload” for the experts, which is a psychological phenomenon causing fatigue and affecting the precision in decision making.³⁶ Hence, the number of shapes must be a trade-off between the benefits of more categories and the costs in observation precision. Behavioral studies have shown that 8 to 15 choices are preferred by consumers and observers.³⁷ Above 15 is considered as “too many”, and below 6 is “too few”.^{38,39} A group of neuroscientists who studied the effects of choice overload on the neural signature in humans stated that 12 items could be perceived as “the right number of options” for human’s visual processing, while six items are “too few” and 24 items are “too many”.⁴⁰

To balance the benefits of more shapes and the costs in observation precision, nine shapes were selected as references: *Fiber*, *rod*, *ellipse*, *oval*, *sphere*, *quadrilateral*, *triangle*, *free-form*, and *unidentifiable*. Strictly speaking, *fiber*, *rod*, and *sphere* describe 3D shapes. However, there is no good term for the 2D projection of *fiber* and *rod*, and they were hence kept as colloquial expressions for their 2D projection. For *sphere*, the 2D projection would be circle. However, we found this to be a somewhat awkward term and hence stayed with using *sphere* as the colloquial expression for this shape. Examples of the pixelized shapes as obtained by FPA- μ FTIR and their idealized geometries are given in Table 1. Particles of at least two adjacent pixels (i.e., $\geq 11 \mu\text{m}$) were considered in this study.^{41–59}

2.3. Experts-Based Shape Evaluation. The five experts were further invited to assess the shapes of the 11,042 microplastics. To differentiate the nine shapes while ensuring flexibility during the assessment, we applied a point allocation method in which the experts were requested to assign a constant sum of points to each particle. This is a common approach in psychophysics and marketing research,⁶¹ where respondents are asked to divide fixed numerical values across multiple attributes or categories to indicate their level of preferences.^{62–64} In physical visualization, the perception of

the objective size was also investigated.⁶⁵ Compared to other survey methods, constant sum scale methods hold the advantage that the respondents are “forced” to make mindful scoring among categories since the total score is fixed, thus allowing the extent of discrimination among attributes to be analyzed statistically.⁶⁶ Typically, the scale has odd-numbered points, for instance, 3, 5, 7, or 11.^{67,68} Though more points can better capture the level of preferences and fine discrimination among categories, the observers may be burdened by mental computation if the number of categories is large, which then may cause fatigue and imprecision.

In our case, each of the five experts had to do the shape scoring for 11,042 particles. Hence, each particle received a point allocation five times. To ease the process and minimize errors, we created a small stand-alone software that automatically opened one image at a time and allowed the expert to score the image into the listed shape categories. The scores were automatically saved on a server and exported as csv for data analysis (Figure S1). Considering the substantial workload, we decided to choose three as the sum of the fixed points to simplify the allocation procedure and reduce the mental computation during observation (Table S1). The indication of specific points is given below, and decimal scoring was not allowed. Before starting to score the images, the experts were gathered and shown a few scoring examples, thus aligning the procedures in scoring. After that, the experts performed the observation separately without discussing with each other; hence, the assessment was not intraobserver influenced. Finally, the “winning shape” was determined as the shape with the highest summed points. Here, we interpreted the results as despite a certain degree of divergence and disagreement, this observed shape was the most similar to that particle’s reference shape. An example of data acquisition and interpretation of the point allocation for one single microplastic from five experts is shown in Table S1.

- 3—the particle looks very much like this shape
- 2—the particle looks like this shape
- 1—the particle looks slightly like this shape
- 0—the particle does not look like this shape

2.4. Data Analysis. **2.4.1. Shape Composition.** Differently shaped microplastics may distribute differently in the environment. To understand such differences, we analyzed the shape composition in each of the seven environmental matrices. Furthermore, the shape composition may vary with the particle size. To investigate this, we sorted the particles into multiple size classes by their major dimensions and calculated the shape composition for each size class. The classes were arranged logarithmically (Figure S2), as microplastics and many other particles in nature are not linearly distributed, as small particles tend to be more abundant than large ones.^{29,60,69}

2.4.2. Divergence and Confusion between Shapes. Due to the subjective perception by humans, divergence and agreement are both anticipated to occur among the experts during the visual shape assessment.^{70,71} We used the standard deviation (STD) of the allocated points as the metric to quantify the level of divergence in perceiving a given shape. An STD value of 0 indicates an absolute agreement, while a higher STD value indicates a higher level of divergence; in other words, the particle is less straightforward to distinguish. An example of interpreting the observation data is given in Supporting Information Table S1.

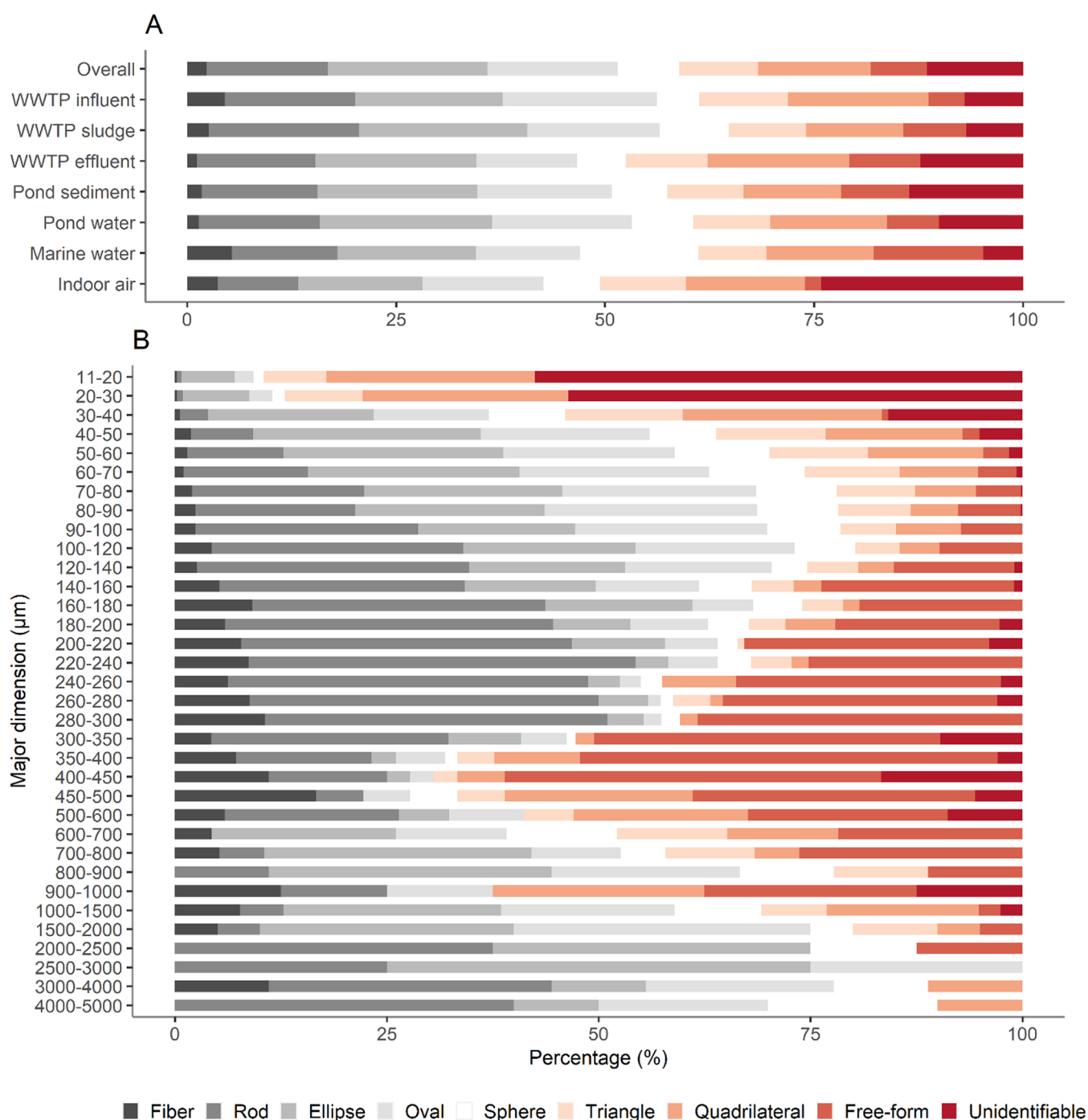


Figure 1. (A) Composition of the nine shape categories was based on visual observation by the five experts for the seven environmental matrices. The overall shape composition after pooling the microplastics from all matrices was termed “Overall”. (B) Shape composition after sorting microplastics into size classes by their major dimension.

When disagreement exists between experts, alternative shapes may cause confusion in differentiating them from the winning shape. Such confusion was illustrated by summing the received scores for each candidate shape and normalizing them to that of the winning shape (Text S1). The normalization was done to make the results among shapes more comparable, as all scores are between 0 and 1 upon normalization. The results were plotted in a heatmap, where a higher score indicates a higher confusion between two associated shapes.

2.4.3. Environmental Microplastics. To understand whether the environmental matrices can cluster by particle

shapes, principal component analysis (PCA) was conducted based on the composition of shape. This was also done for the particle size. The size refers to the particle's major dimension; it was logarithmized and sorted into bins of 0.2 widths.¹⁷ When referring to bin sizes, the average size is stated; e.g., the bin from 1 to 1.2 is referred to as 1.1. All statistics were done in R (v 3.6.3).

3. RESULTS

3.1. Microplastic Shape Composition. Lumping all 11,042 microplastics, *ellipse* was the most abundant (19.1%)

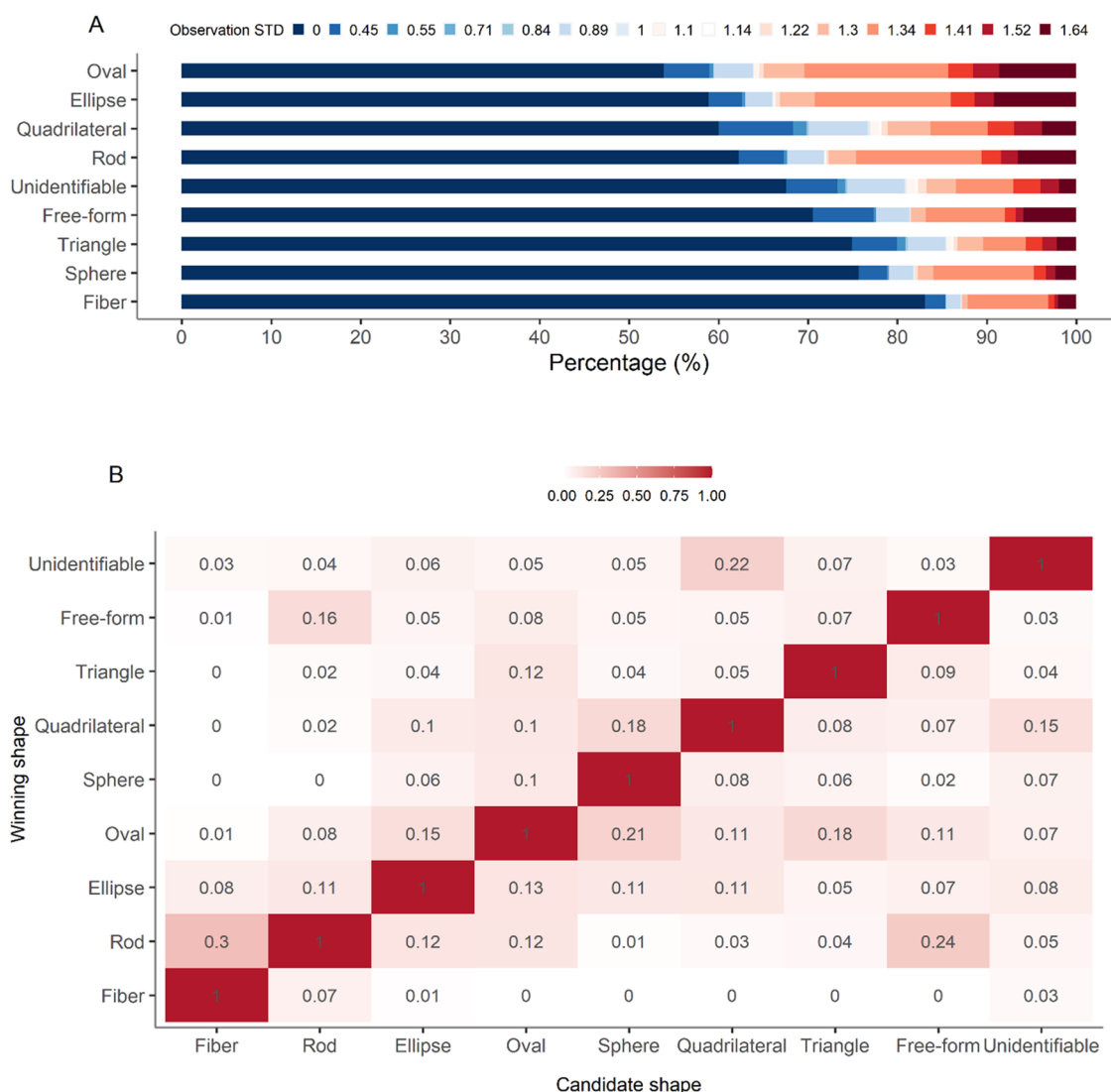


Figure 2. (A) Standard deviations (STD) on agreements for each proposed shape category. (B) Heatmap of the obtained scores for each proposed shape. The y-axis lists the winning shapes (overall determined shape by the experts), and the values in the rows indicate the degree of confusion caused by shapes that are alternative to the winning shape.

followed by *oval* (15.6%) and *rod* (14.5%), while *fiber* was the least abundant (2.3%, Figure 1A, Table S2). When the shapes in each environmental matrix were compared, *fiber* again was the least abundant, except in marine water where it was the second least common shape. In contrast, *ellipse*, *oval*, and *rod* are the top three most abundant shapes.

When looking at *fiber* among the WWTP-related samples (influent, effluent, and sludge), effluent held less (1.0%) compared with influent (4.2%) and sludge (2.6%). In contrast, an increase of 4.4% in *unidentifiable* was seen in the effluent compared to the influent. The highest fraction (24.1%) of *unidentifiable* was detected in indoor air. As for the stormwater-associated matrices, all shapes were equally distributed between the stormwater and sediments.

Particle shapes depended on the particle size (Figure 1B, Table S3). The frequency of the two most elongated shapes, *fiber* and *rod*, exhibited a clear trend of increase from 11 to 300 μm . The trend was steepest for *rod*, which peaked at 220–240 μm with a frequency of 45.6%. The rising trend was also seen in *free-form* from 30 to 400 μm . *Unidentifiable* dominated in the two smallest size classes: 11–20 μm (57.5%) and 20–30

μm (53.6%). Notably, 92.3% of the microplastics were ≤ 200 μm , among which the fraction of 30–40 μm held most of the particles, namely, 16.4%.

3.2. Divergence and Confusion in Shape Perception.

Both absolute agreement (STD = 0) and strong disagreement (STD = 1.64) were observed among the five experts (Figure 2A, Table S4). *Fiber* received the highest composition of absolute agreement (83.1%), followed by *sphere* (75.7%). Contrarily, *ellipse* and *oval* had the lowest absolute agreement (59 and 54%, respectively) and a high frequency of strong disagreement (9.2 and 8.3%).

Overall, all proposed shapes could be sufficiently distinguished since the highest confusion value was only 0.3 (*fiber* versus *rod*) (Figure 2B). However, *rod* versus *fiber*, and *rod* versus *free-form* exhibited slight pairwise confusion, with confusion values of 0.30 and 0.24 when *rod* was the winning shape. In other words, *fiber* and *free-form* caused confusion among the observers when differentiating them from *rod*. *Oval* caused 0.21 of confusion for *sphere*, and 0.15 for *ellipse*. Furthermore, *unidentifiable* caused a confusion of 0.22 toward *quadrilateral*.

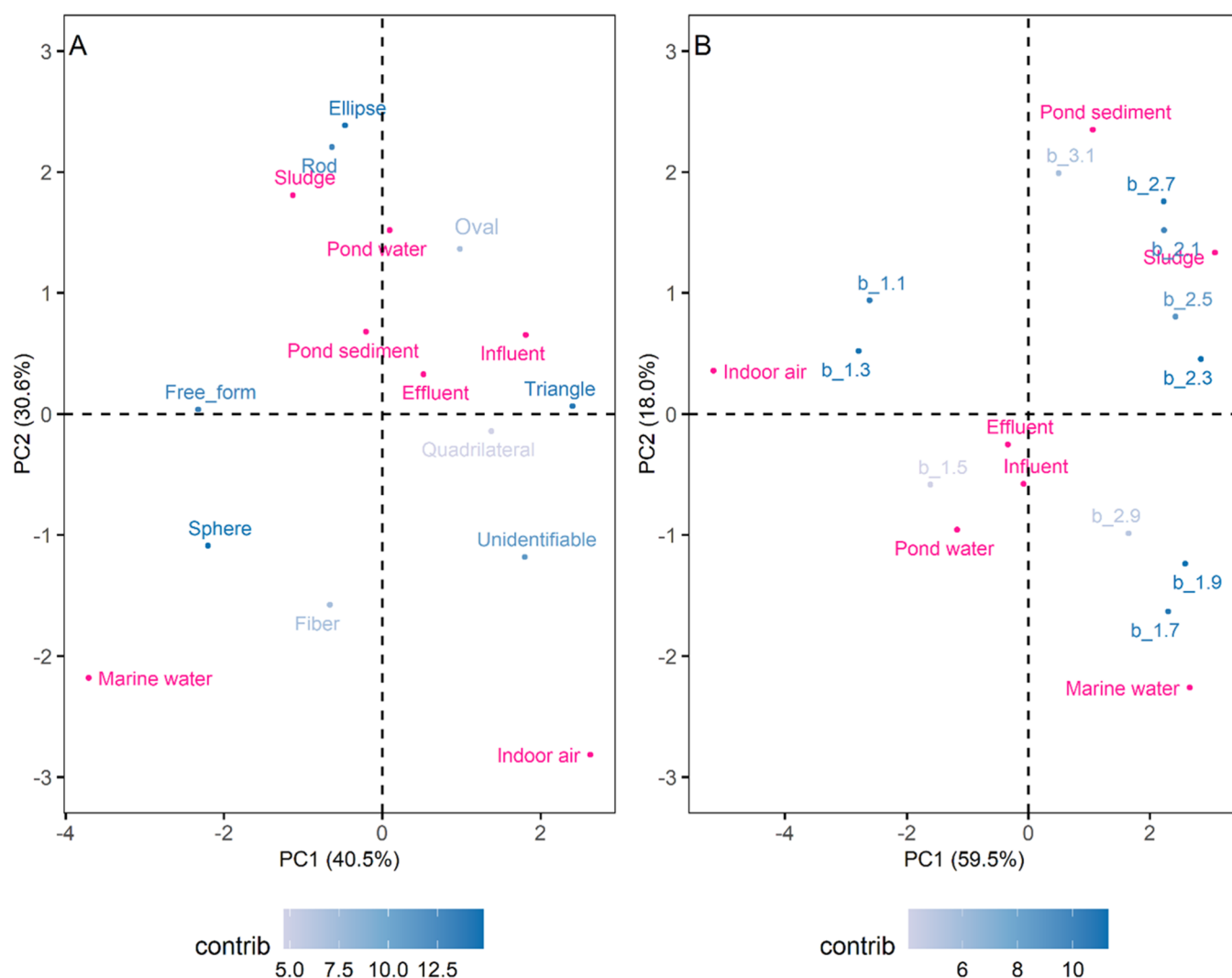


Figure 3. PCA of particle shape (A) and size (B) of microplastics from the seven environmental matrices (pink). The contribution of each variable is visualized by its shade of blue (the darker, the higher the contribution). The variables in (B) are logarithmized major dimensions and binned into step widths of 0.2, written as *b_* followed by the logarithmized length.

3.3. Environmental Microplastics. Three distinct clusters were identified among the shapes from the seven matrices: freshwater compartment, including stormwater (i.e., pond water, pond sediment), and WWTP (i.e., influent, effluent, sludge) clustered as one group, while both indoor air and marine water self-grouped (Figure 3a). Here, the first principal component (PC1) explained 40.5% of the variation and PC2 explained 30.6%. The self-grouping of indoor air was mainly driven by a high frequency of *unidentifiable*, and for marine water, by a high frequency of *sphere*. The clustering of stormwater and WWTP-associated sources was explained by their shared high frequency of *ellipse* and *rod*.

A phase-based clustering was seen with respect to the particle size (Figure 3b). Indoor air again, self-grouped due to a high frequency of small particles, particularly bins 1.1 and 1.3 (corresponding to mean sizes up to 20 μm). Water samples (WWTP influent and effluent, stormwater, marine water) clustered by a high frequency of medium-sized bins 1.5 and 1.7 (corresponding to 32 and 50 μm mean size, respectively). Solid samples (WWTP sludge, pond sediments) clustered as a group driven by a high proportion of large-sized bins of 2.1 and

3.1 (corresponding to mean sizes of 126 and 1259 μm , respectively).

4. DISCUSSION

4.1. Shape Categories for the Imaged Microplastics.

Shape categories of imaged microplastics tend to lack precise definitions, and many studies apply categories that cannot be rigorously defined, inevitably leading to ambiguous shape classification and incomparability across data. For instance, *fragment* was used to represent shapes other than *fiber*, *film*, and *pellet*,⁷² while in another study, the term *fragment* was applied for shapes other than *fiber* and *bead*.⁷³ Although neither of them gave a clear definition of the shape of a *fragment*, they used the term to cover different shapes.

Some studies proposed better-defined shape categories, for instance, Hartmann et al.²⁰ defined *film* as planar particles with one dimension significantly smaller than the other two, but such a shape was only suggested for particles >300 μm . This leaves particles $\leq 300 \mu\text{m}$ with only three shape options: *sphere*, *fiber*, and *irregular*. *Fiber* by the same study was defined as particles with one dimension significantly longer than the other two.²⁰ Such particles, whether analyzed by optical (3D images)

or hyperspectral imaging (2D images), can rather straightforwardly be identified as *fiber*, or other very elongated shapes, for instance, *rod*. Another study⁷⁴ recommended three core shape groups: *beads*, *fibers*, and *fragments*, and suggested further subcategorization if more detailed properties can be recorded. It must be pointed out that such core shapes targeted more on microplastics being visually identified, namely, 3D images, rather than 2D images.

To avoid such ambiguity and generate more comparable data across studies applying hyperspectral imaging, we propose a set of shape categories with explicit definitions. The objective of the stringent definition is to make each shape unique and allow the observer to have clear rules to refer to when sorting particles into shape bins. The selection of such shapes was intended to represent the most environmentally relevant microplastic shapes and at the same to comprise a number of categories within the optimal range for human visual processing,³⁷ hereby ensuring feasibility and precision in manual shape assessment. Compared with the existing shape categories in the field, which might contain a mix of 2D and 3D images, we believe that the shapes proposed in this study can strengthen and enrich the morphological description of microplastics. For instance, if a particle meets the definition of *film* (3D) while having the top projection as circular (2D), then its morphology can be described as “a *film* with *sphere*-shaped planar projection”. This echoes the concept of core and subcategories recommended by Lusher et al.,⁷⁴ together leading to a more comprehensive morphological description.

The proposed shapes were very distinguishable to the human eye, especially the most/least elongated shapes: *fiber* and *sphere*. Their high distinguishability was in line with another study stating that the human eye is more sensitive toward “extremely formed” shapes.⁷⁵ Minor confusion existed for *oval* versus *sphere* and *ellipse*, which could be explained by the fact that despite all being rounded and less elongated, the degree of symmetry varied yet the visual perception of symmetry could vary between individuals. Confusion was also found for *rod* versus *free-form* and *fiber*. *Free-form*, defined as having uneven curves and angular contours, can at the same time be elongated, at which point it becomes difficult for an expert to perceive its overall angularity, which, in principle, would differentiate it from *rod*. *Fiber* was defined as particles having a constant diameter along the longest skeleton; however, when a particle is highly elongated, some fluctuation in diameter along the length of the particle is less discernible to the human eye, leading to confusion between *rod* and *fiber*. Furthermore, the confusion between *unidentifiable* and *quadri-lateral* suggested that the number of pixels constituting a particle can affect the human perception of a particle's angularity.

The shapes proposed here are not aimed to be the ultimate set of categories for imaged microplastics but are intended to show the importance of choosing rigorous shape categories when reporting the shape of microplastics. In a different context, a different set of shape choices may be appropriate. Take *ellipse* and *oval* as an example, if the degree of symmetry is not of interest, one could merge them to avoid confusion, at the same time speeding up the categorization. Same goes for *fiber* and *rod*, which could be merged if the diameter fluctuation along the particle's skeleton is not of interest (Table 1). What however is important is to set clear shape definitions and evaluate their distinguishability by manual assessment before applying them to actual samples.

4.2. Environmental Microplastics. **4.2.1. Shape of Microplastics.** *Rod*, *ellipse*, and *oval* were the most abundant shapes of microplastics regardless of the environmental matrix. The shapes have two geometric characteristics in common: they are less elongated and more rounded. This could be associated with weathering and abrasion,^{76–78} as both are processes that could make angular edges of microplastics more rounded.

Comparing the shape frequencies of this study to other data is not straightforward, as many applied broader categories, e.g., *fragment* and *irregular* without giving clear definitions, and often found that these shapes dominated in the environment.^{79–81} In this study, *fiber* was the least abundant shape, which seems in conflict with many studies stating that *fiber* is the most common shape in the environment. For example, in the Himalayas⁸² and in wild-caught Mediterranean mussels.⁸³ Many studies applying manual sorting under a microscope combined with chemical identification (e.g., FTIR) concluded that the *fiber* is the most common shape. However, manual sorting tends to bias toward visually recognizable microplastics, mainly fibers and larger fragments. High-resolution hyperspectral imaging, on the other hand, does not have such sorting bias and can reach lower sizes. As small microplastics are much more abundant than larger ones, this leads to *fibers* often being less common in hyperspectral imaging. In addition, and a fact seldom stated by studies using such imaging, *fibers* tend to not lie flat on the substratum to be scanned, hence, going in and out of the focal plane of the instrument. This leads to poorer spectra when the fiber is out of focus, which can lead to it being seen as several separate particles.⁸⁴ The same can be an issue if a particle has an uneven thickness. For instance, over 7% of 60,000 microplastics down to 11–20 μm were found to be *fiber*.⁸⁵ As it stands, we believe neither result is inherently wrong, and the differences mainly must be attributed to the different techniques applied, which inevitably bring different biases and de facto size quantification limits.

Microplastics from freshwater compartment (incl. storm-water and WWTPs) clustered due to a high frequency of *ellipse* and *rod*. Other studies found other results. For example, *fragment* (52.4%) and *fiber* (32.5%) were the most common shapes of microplastics in urban river waters in China, by applying a stereomicroscope combined with LDIR.⁸¹ While the category *fragment* carries little information about shape and comparison to the shapes applied in the present study hence is problematic, the category *fiber* should be rather comparable. However, no definition of what distinguished a *fragment* from a *fiber* was given.

It was also evident that microplastic shapes depended on the particle size. Small particles consisting of a few pixels made the shape abstract (*unidentifiable*) hence hard to describe in geometric terms. Similar results were reported by another study, stating that it is not possible to identify the shape of particles made of a single or a few pixels.⁷³ When the particle size and thereby the number of pixels increase, it is more likely to reveal its shape. In the end, it is crucial to give a defined category to such shape, as the majority of microplastics found in the environment are small and numbers hence tend to increase toward the lower size detection limit of the applied analytical technique. With the pixel resolution of 11 μm , the majority of microplastics were $\leq 100 \mu\text{m}$.^{60,86}

4.2.2. Size of Microplastics. The relation between the particle size and matrix can be associated with their fate and transport in the environment. Larger particles, for instance,

which tend to be heavier in mass, are more likely to settle, while smaller ones have a better chance to be carried by flowing waters and wind. This means that they have a higher likelihood to be transported over long distances, for example, within the atmosphere. Applying the hyperspectral imaging technique and the same cutoff size limit ($11\ \mu\text{m}$) as the current study, it was found that 80% of the microplastics in snow from the Alps to the Arctic were $\leq 25\ \mu\text{m}$,⁸⁷ which echoed the current study, both implying that smaller particles are subjected to transport over longer distances.

It must be pointed out that the difference between environmental compartments elucidated by particle shape and size has certain limitations in revealing the actual transport of microplastic as different compartments are likely subjected to different sources and transport mechanisms, which affect the ultimate occurrence of microplastics in the environment. Within the same compartment, reflections on how the particle transport mechanisms and fate relate to the size and shape seem more reliable. Taking the WWTP-related matrices as an example, *fiber* decreased from influent (4.2%) to effluent (1.0%); contrarily, the smallest particle, namely, *unidentifiable*, increased (7.8% in influent, 12.2% in effluent, Table S2). Not to mention, sludge held most of the largest particles. This signifies that bigger particles like *fiber* were retained rather efficiently by the WWTP, while smaller ones had a higher probability of being released with the effluents. The question of whether such small particles originate from the source or are formed by fragmentation from bigger particles during the treatment however remains. Another water compartment, stormwater, and sediments from stormwater ponds revealed a similar pattern, namely, that larger particles were more likely to deposit, while smaller ones tended to float. A similar observation was reported in over 60,000 microplastics detected in samples from different aquatic compartments; it states that within the same compartment, sediments held larger microplastics than waters, and that it held true both for marine and freshwater compartments.⁸⁸ All of these results seem to point in the same direction, namely, that within the same environmental compartment, microplastic size, at least to some degree, drives the transport and determines their eventual fate in the environment.

5. IMPLICATIONS

Subjective divergence and confusion cannot be avoided when manual inspection is applied to categorize shapes. A purely mathematical approach does not have such limitations and benefits from applying a more robust and reproducible classifier. Computers furthermore experience fatigue and can readily apply mathematical routines to derive parameters, such as sphericity, angularity, and roughness, which can be derived mathematically from the image. However, these often carry little intuitive meaning to humans. It often makes more sense to apply shape categories that make sense to the human eye and which are clearly distinguishable by humans. The observation data of our study could serve as the “ground truth” to train a mathematical model against a set of such shape categories. Once established, such a model would function independently of the number of microplastics to be analyzed. However, it would rely heavily on the quality of training data, as biased training data would inevitably produce a biased model.⁸⁹ Good training data serving as the “ground truth” is hence essential, which should be as unambiguous as possible. To reduce the ambiguity of the shape categories, one could

merge the less distinguishable shapes. In any case, the first choice must be the shape categories against which to train up, and we hope this study can give inspiration regarding what to consider and some of the pitfalls in this respect.

■ ASSOCIATED CONTENT

Supporting Information

The Supporting Information is available free of charge at <https://pubs.acs.org/doi/10.1021/acs.est.3c03517>.

Example of data acquisition and interpretation of the point allocation method in manual shape evaluation; shape composition sorted by environmental matrix and size classes; distribution of size for each shape; composition of STD in shape evaluation; and correlation between variables and PC both for particle shape and size analysis (PDF)

■ AUTHOR INFORMATION

Corresponding Author

Fan Liu – Department of the Built Environment, Aalborg University, 9220 Aalborg Ø, Denmark; orcid.org/0000-0002-7975-4790; Email: fl@build.aau.dk

Authors

Lasse A. Rasmussen – Department of the Built Environment, Aalborg University, 9220 Aalborg Ø, Denmark

Nanna D. R. Klemmensen – Department of the Built Environment, Aalborg University, 9220 Aalborg Ø, Denmark

Guohan Zhao – Research Centre for Built Environment, Energy, Water and Climate, VIA University College, 8700 Horsens, Denmark

Rasmus Nielsen – Department of the Built Environment, Aalborg University, 9220 Aalborg Ø, Denmark; orcid.org/0000-0002-3819-4555

Alvise Vianello – Department of the Built Environment, Aalborg University, 9220 Aalborg Ø, Denmark

Sinja Rist – National Institute of Aquatic Resources, Technical University of Denmark, 2800 Kongens Lyngby, Denmark

Jes Vollertsen – Department of the Built Environment, Aalborg University, 9220 Aalborg Ø, Denmark

Complete contact information is available at:

<https://pubs.acs.org/doi/10.1021/acs.est.3c03517>

Notes

The authors declare no competing financial interest.

■ ACKNOWLEDGMENTS

This work was funded by MarinePlastic (Project no. 25084). The authors thank Rupa Chand for helping with testing the preliminary version of the shape assessment method.

■ REFERENCES

- (1) Afrin, S.; Rahman, M. M.; Akbor, M. A.; Siddique, M. A. B.; Uddin, M. K.; Malafaia, G. Is There Tea Complemented with the Appealing Flavor of Microplastics? A Pioneering Study on Plastic Pollution in Commercially Available Tea Bags in Bangladesh. *Sci. Total Environ.* **2022**, 837, 155833.
- (2) Goßmann, I.; Süßmuth, R.; Scholz-Böttcher, B. M. Plastic in the Air?! - Spider Webs as Spatial and Temporal Mirror for Microplastics Including Tire Wear Particles in Urban Air. *Sci. Total Environ.* **2022**, 832, 155008.
- (3) Grillo, J. F.; López-Ordaz, A.; Hernández, A. J.; Catari, E.; Sabino, M. A.; Ramos, R. Synthetic Microfiber Emissions from Denim

Industrial Washing Processes: An Overlooked Microplastic Source within the Manufacturing Process of Blue Jeans. *Sci. Total Environ.* **2023**, 884, No. 163815.

(4) Kaur, M.; Ghosh, D.; Guleria, S.; Arya, S. K.; Puri, S.; Khatri, M. Microplastics/Nanoplastics Released from Facemasks as Contaminants of Emerging Concern. *Mar. Pollut. Bull.* **2023**, 191, No. 114954.

(5) Schwarzer, M.; Brehm, J.; Vollmer, M.; Jasinski, J.; Xu, C.; Zainuddin, S.; Fröhlich, T.; Schott, M.; Greiner, A.; Scheibel, T.; Laforsch, C. Shape, Size, and Polymer Dependent Effects of Microplastics on *Daphnia Magna*. *J. Hazard Mater.* **2022**, 426, 128136.

(6) Zhang, M.; Xu, D.; Liu, L.; Wei, Y.; Gao, B. Vertical Differentiation of Microplastics Influenced by Thermal Stratification in a Deep Reservoir. *Environ. Sci. Technol.* **2023**, 57 (17), 6999–7008.

(7) Coyle, R.; Service, M.; Witte, U.; Hardiman, G.; McKinley, J. Modeling Microplastic Transport in the Marine Environment: Testing Empirical Models of Particle Terminal Sinking Velocity for Irregularly Shaped Particles. *ACS ES&T Water* **2023**, 3 (4), 984–995, DOI: 10.1021/acsestwater.2c00466.

(8) Yu, Z.; Yang, G.; Zhang, W. A New Model for the Terminal Settling Velocity of Microplastics. *Mar. Pollut. Bull.* **2022**, 176 (February), No. 113449.

(9) Long, X.; Fu, T. M.; Yang, X.; Tang, Y.; Zheng, Y.; Zhu, L.; Shen, H.; Ye, J.; Wang, C.; Wang, T.; Li, B. Efficient Atmospheric Transport of Microplastics over Asia and Adjacent Oceans. *Environ. Sci. Technol.* **2022**, 56, 6243.

(10) Amaral-Zettler, L. A.; Zettler, E. R.; Mincer, T. J.; Klaassen, M. A.; Gallagher, S. M. Biofouling Impacts on Polyethylene Density and Sinking in Coastal Waters: A Macro/Micro Tipping Point? *Water Res.* **2021**, 201, No. 117289.

(11) Ding, R.; Ouyang, Z.; Zhang, X.; Dong, Y.; Guo, X.; Zhu, L. Biofilm-Colonized versus Virgin Black Microplastics to Accelerate the Photodegradation of Tetracycline in Aquatic Environments: Analysis of Underneath Mechanisms. *Environ. Sci. Technol.* **2023**, 57, 5714–5725.

(12) Sun, B.; Hu, Y.; Cheng, H.; Tao, S. Releases of Brominated Flame Retardants (BFRs) from Microplastics in Aqueous Medium: Kinetics and Molecular-Size Dependence of Diffusion. *Water Res.* **2019**, 151, 215–225.

(13) Munoz, M.; Ortiz, D.; Nieto-Sandoval, J.; de Pedro, Z. M.; Casas, J. A. Adsorption of Micropollutants onto Realistic Microplastics: Role of Microplastic Nature, Size, Age, and NOM Fouling. *Chemosphere* **2021**, 283, No. 131085.

(14) Cowger, W.; Booth, A. M.; Hamilton, B. M.; Thaysen, C.; Primpke, S.; Munno, K.; Lusher, A. L.; Dehaut, A.; Vaz, V. P.; Liboiron, M.; Devriese, L. I.; Hermabessiere, L.; Rochman, C.; Athey, S. N.; Lynch, J. M.; De Frond, H.; Gray, A.; Jones, O. A. H.; Brander, S.; Steele, C.; Moore, S.; Sanchez, A.; Nel, H. Reporting Guidelines to Increase the Reproducibility and Comparability of Research on Microplastics. *Appl. Spectrosc.* **2020**, 74 (9), 1066–1077.

(15) Vasanthi, R. L.; Arulvasu, C.; Kumar, P.; Srinivasan, P. Ingestion of Microplastics and Its Potential for Causing Structural Alterations and Oxidative Stress in Indian Green Mussel *Perna Viridis*—A Multiple Biomarker Approach. *Chemosphere* **2021**, 283 (February), No. 130979.

(16) Simon, M.; van Alst, N.; Vollertsen, J. Quantification of Microplastic Mass and Removal Rates at Wastewater Treatment Plants Applying Focal Plane Array (FPA)-Based Fourier Transform Infrared (FT-IR) Imaging. *Water Res.* **2018**, 142, 1–9.

(17) Liu, F.; Olesen, K. B.; Borregaard, A. R.; Vollertsen, J. Microplastics in Urban and Highway Stormwater Retention Ponds. *Sci. Total Environ.* **2019**, 671, 992–1000.

(18) Molazadeh, M.; Liu, F.; Simon-Sánchez, L.; Vollersten, J. Buoyant Microplastics in Freshwater Sediments – How Do They Get There? *Sci. Total Environ.* **2023**, 860, No. 160489.

(19) Valls-Conesa, J.; Winterauer, D. J.; Kröger-Lui, N.; Roth, S.; Liu, F.; Lüttjohann, S.; Harig, R.; Vollertsen, J. Random Forest Microplastic Classification Using Spectral Subsamples of FT-IR Hyperspectral Images. *Anal. Methods* **2023**, 15, 2226.

(20) Hartmann, N. B.; Hüffer, T.; Thompson, R. C.; Hassellöv, M.; Verschoor, A.; Daugaard, A. E.; Rist, S.; Karlsson, T.; Brennholt, N.; Cole, M.; Herrling, M. P.; Hess, M. C.; Ivleva, N. P.; Lusher, A. L.; Wagner, M. Are We Speaking the Same Language? Recommendations for a Definition and Categorization Framework for Plastic Debris. *Environ. Sci. Technol.* **2019**, 53 (3), 1039–1047.

(21) Shi, B.; Patel, M.; Yu, D.; Yan, J.; Li, Z.; Petriw, D.; Pruyn, T.; Smyth, K.; Passeport, E.; Miller, R. J. D.; Howe, J. Y. Automatic Quantification and Classification of Microplastics in Scanning Electron Micrographs via Deep Learning. *Sci. Total Environ.* **2022**, 825, 153903.

(22) Naderi Beni, N.; Karimifard, S.; Gilley, J.; Messer, T.; Schmidt, A.; Bartelt-Hunt, S. Higher Concentrations of Microplastics in Runoff from Biosolid-Amended Croplands than Manure-Amended Croplands. *Commun. Earth Environ.* **2023**, 4 (1), 42.

(23) Zheng, J.; Hryciw, R. D. Traditional Soil Particle Sphericity, Roundness and Surface Roughness by Computational Geometry. *Geotechnique* **2015**, 65 (6), 494–506.

(24) Aust, A. E.; Cook, P. M.; Dodson, R. F. Morphological and Chemical Mechanisms of Elongated Mineral Particle Toxicities. *J. Toxicol. Environ. Health, Part B* **2011**, 14, 40–75.

(25) Berrezueta, E.; Cuervas-Mons, J.; Rodríguez-Rey, Á.; Ordóñez-Casado, B. Representativity of 2D Shape Parameters for Mineral Particles in Quantitative Petrography. *Minerals* **2019**, 9 (12), 768.

(26) Powers, M. C. A New Roundness Scale for Sedimentary Particles. *SEPM J. Sediment. Res.* **1953**, 23 (2), 117–119.

(27) Sims, I.; Lay, J.; Ferrari, J. I. Concrete Aggregates. In *Lea's Chemistry of Cement and Concrete*, Butterworth-Heinemann, 2019; pp 699–778.

(28) Rist, S.; Vianello, A.; Winding, M. H. S.; Nielsen, T. G.; Almeda, R.; Torres, R. R.; Vollertsen, J. Quantification of Plankton-Sized Microplastics in a Productive Coastal Arctic Marine Ecosystem. *Environ. Pollut.* **2020**, 266, 115248.

(29) Simon, M.; Van Alst, N.; Vollertsen, J. Quantification of Microplastic Mass and Removal Rates at Wastewater Treatment Plants Applying Focal Plane Array (FPA)-Based Fourier Transform Infrared (FT-IR) Imaging. *Water Res.* **2018**, 142, 1–9.

(30) Rasmussen, L. A.; Iordachescu, L.; Tumlin, S.; Vollertsen, J. A Complete Mass Balance for Plastics in a Wastewater Treatment Plant Macroplastics Contributes More than Microplastics. *Water Res.* **2021**, 201, No. 117307.

(31) Liu, F.; Vianello, A.; Vollertsen, J. Retention of Microplastics in Sediments of Urban and Highway Stormwater Retention Ponds. *Environ. Pollut.* **2019**, 255, 113335.

(32) Vianello, A.; Jensen, R. L.; Liu, L.; Vollertsen, J. Simulating Human Exposure to Indoor Airborne Microplastics Using a Breathing Thermal Manikin. *Sci. Rep.* **2019**, 9 (1), No. 8670.

(33) Primpke, S.; Cross, R. K.; Mintenig, S. M.; Simon, M.; Vianello, A.; Gerdts, G.; Vollertsen, J. Toward the Systematic Identification of Microplastics in the Environment: Evaluation of a New Independent Software Tool (SiMPle) for Spectroscopic Analysis. *Appl. Spectrosc.* **2020**, 74, 1127–1138.

(34) Ikart, E. M. Survey Questionnaire Survey Pretesting Method: An Evaluation of Survey Questionnaire via Expert Reviews Technique. *Asian J. Social Sci. Studies* **2019**, 4 (2), 1.

(35) O Nyumba, T.; Wilson, K.; Derrick, C. J.; Mukherjee, N. The Use of Focus Group Discussion Methodology: Insights from Two Decades of Application in Conservation. *Methods Ecol. Evol.* **2018**, 9 (1), 20–32.

(36) Scheibehenne, B.; Greifeneder, R.; Todd, P. M. Can There Ever Be Too Many Options? A Meta-Analytic Review of Choice Overload. *J. Consumer Res.* **2010**, 37 (3), 409–425.

(37) Reutskaja, E.; Lindner, A.; Nagel, R.; Andersen, R. A.; Camerer, C. F. Choice Overload Reduces Neural Signatures of Choice Set Value in Dorsal Striatum and Anterior Cingulate Cortex. *Nat. Human Behaviour.* **2018**, 2, 925–935.

(38) Shah, A. M.; Wolford, G. Buying Behavior as a Function of Parametric Variation of Number of Choices: Short Report. *Psychol. Sci.* **2007**, 18, 369–370.

- (39) Reutskaja, E.; Hogarth, R. M. Satisfaction in Choice as a Function of the Number of Alternatives: When “Goods Satiates.” *Psychol. Mark.* **2009**, *26* (3), 197–203.
- (40) Reutskaja, E.; Lindner, A.; Nagel, R.; Andersen, R. A.; Camerer, C. F. Choice Overload Reduces Neural Signatures of Choice Set Value in Dorsal Striatum and Anterior Cingulate Cortex. *Nat. Human Behaviour*. **2018**, *2*, 925–935.
- (41) Sun, Y.; Cai, Z.; Fu, J. Particle Morphomics by High-Throughput Dynamic Image Analysis. *Sci. Rep.* **2019**, *9* (1), No. 9591.
- (42) Aust, A. E.; Cook, P. M.; Dodson, R. F. Morphological and Chemical Mechanisms of Elongated Mineral Particle Toxicities. *J. Toxicol. Environ. Health, Part B* **2011**, *14* (1–4), 40–75.
- (43) Cai, Y.; Yang, T.; Mitrano, D. M.; Heuberger, M.; Hufenus, R.; Nowack, B. Systematic Study of Microplastic Fiber Release from 12 Different Polyester Textiles during Washing. *Environ. Sci. Technol.* **2020**, *54*, 4847.
- (44) Bratton, B. P.; Shaevitz, J. W.; Gitai, Z.; Morgenstein, R. M. MreB Polymers and Curvature Localization Are Enhanced by RodZ and Predict E. Coli’s Cylindrical Uniformity. *Nat. Commun.* **2018**, *9* (1), No. 2797, DOI: [10.1038/s41467-018-05186-5](https://doi.org/10.1038/s41467-018-05186-5).
- (45) Su, L.; Sharp, S. M.; Pettigrove, V. J.; Craig, N. J.; Nan, B.; Du, F.; Shi, H. Superimposed Microplastic Pollution in a Coastal Metropolis. *Water Res.* **2020**, *168*, 115140.
- (46) Blott, S. J.; Pye, K. Particle Shape: A Review and New Methods of Characterization and Classification. *Sedimentology* **2008**, *55* (1), 31–63.
- (47) Kinloch, A. J.; Taylor, C. The Toughening of Cyanate-Ester Polymers. Part I Physical Modification Using Particles, Fibres and Woven-Mats. *J. Mater. Sci.* **2002**, *37* (3), 433–460.
- (48) Persson, A. L. Image Analysis of Shape and Size of Fine Aggregates. *Eng. Geol.* **1998**, *50* (1–2), 177–186.
- (49) Takashimizu, Y.; Iiyoshi, M. New Parameter of Roundness R: Circularity Corrected by Aspect Ratio. *Prog. Earth Planet Sci.* **2016**, *3* (1), 2 DOI: [10.1186/s40645-015-0078-x](https://doi.org/10.1186/s40645-015-0078-x).
- (50) Bray, D. J.; Gilmour, S. G.; Guild, F. J.; Taylor, A. C. The Effects of Particle Morphology on the Analysis of Discrete Particle Dispersion Using Delaunay Tessellation. *Composites, Part A* **2013**, *54*, 37–45.
- (51) Gaston, E.; Woo, M.; Steele, C.; Sukumaran, S.; Anderson, S. Microplastics Differ Between Indoor and Outdoor Air Masses: Insights from Multiple Microscopy Methodologies. *Appl. Spectrosc.* **2020**, *74* (9), 1079–1098.
- (52) Berrezueta, E.; Cuervas-Mons, J.; Rodríguez-Rey, Á.; Ordóñez-Casado, B. Representativity of 2D Shape Parameters for Mineral Particles in Quantitative Petrography. *Minerals* **2019**, *9* (12), 768.
- (53) Waldschläger, K.; Schüttrumpf, H. Infiltration Behavior of Microplastic Particles with Different Densities, Sizes, and Shapes-From Glass Spheres to Natural Sediments. *Environ. Sci. Technol.* **2020**, *54* (15), 9366–9373.
- (54) Sobhani, Z.; Lei, Y.; Tang, Y.; Wu, L.; Zhang, X.; Naidu, R.; Megharaj, M.; Fang, C. Microplastics Generated When Opening Plastic Packaging. *Sci. Rep.* **2020**, *10* (1), 4841 DOI: [10.1038/s41598-020-61146-4](https://doi.org/10.1038/s41598-020-61146-4).
- (55) Wessol, D. E.; Wheeler, F. J. Creating and Using a Type of Free-Form Geometry in Monte Carlo Particle Transport. *Nucl. Sci. Eng.* **1993**, *113* (4), 314–323.
- (56) Vatavu, A.; Danescu, R.; Nedevschi, S. Stereovision-Based Multiple Object Tracking in Traffic Scenarios Using Free-Form Obstacle Delimiters and Particle Filters. *IEEE Trans. Intell. Transp. Syst.* **2015**, *16* (1), 498–511.
- (57) Spröte, P.; Schmidt, F.; Fleming, R. W. Visual Perception of Shape Altered by Inferred Causal History. *Sci. Rep.* **2016**, *6*, 36245 DOI: [10.1038/srep36245](https://doi.org/10.1038/srep36245).
- (58) Doskolovich, L. L.; Dmitriev, A. Y.; Bezus, E. A.; Moiseev, M. A. Analytical Design of Freeform Optical Elements Generating an Arbitrary-Shape Curve. *Appl. Opt.* **2013**, *52* (12), 2521–2526.
- (59) Torralba, A. How Many Pixels Make an Image? *Vis. Neurosci.* **2009**, *26* (1), 123–131.
- (60) Rolf, M.; Laermanns, H.; Kienzler, L.; Pohl, C.; Möller, J. N.; Laforsch, C.; Löder, M. G. J.; Bogner, C. Flooding Frequency and Floodplain Topography Determine Abundance of Microplastics in an Alluvial Rhine Soil. *Sci. Total Environ.* **2022**, 836 (December 2021), 155141 DOI: [10.1016/j.scitotenv.2022.155141](https://doi.org/10.1016/j.scitotenv.2022.155141).
- (61) Stevens, S. S. Issues in Psychophysical Measurement. *Psychol. Rev.* **1971**, *78* (5), 426–450.
- (62) Stevens, S. S. On the Theory of Scales of Measurement. *Science* **1946**, *103* (2684), 677–680.
- (63) Schaie, K. W. Scaling the Scales: Use of Expert Judgment in Improving the Validity of Questionnaire Scales. *J. Consult. Psychol.* **1963**, *27* (4), 350–357.
- (64) Louviere, J. J.; Islam, T. A Comparison of Importance Weights and Willingness-to-Pay Measures Derived from Choice-Based Conjoint, Constant Sum Scales and Best-Worst Scaling. *J. Bus. Res.* **2008**, *61* (9), 903–911.
- (65) Jansen, Y.; Hornbaek, K.; Kasper, H. A Psychophysical Investigation of Size as a Physical Variable. *IEEE Trans. Vis. Comput. Graph.* **2016**, *22* (1), 479–488, DOI: [10.1109/TVCG.2015.2467951](https://doi.org/10.1109/TVCG.2015.2467951).
- (66) Johnson, R. M. Electronic Questionnaire Design and Analysis with CAPP. *J. Marketing Res.* **1986**, *23* (1), 83–85.
- (67) Dawes, J. Do Data Characteristics Change According to the Number of Scale Points Used? An Experiment Using 5-Point, 7-Point and 10-Point Scales. *Int. J. Market Res.* **2008**, *50* (1), 61–77.
- (68) De Beuckelaer, A.; Toonen, S.; Davidov, E. On the Optimal Number of Scale Points in Graded Paired Comparisons. *Qual. Quant.* **2013**, *47* (5), 2869–2882.
- (69) Haave, M.; Lorenz, C.; Primpke, S.; Gerdt, G. Different Stories Told by Small and Large Microplastics in Sediment - First Report of Microplastic Concentrations in an Urban Recipient in Norway. *Mar. Pollut. Bull.* **2019**, *141* (February), 501–513.
- (70) Cull, W. L.; O’Connor, K. G.; Sharp, S.; Tang, S. F. S. Response Rates and Response Bias for 50 Surveys of Pediatricians. *Health Serv. Res.* **2005**, *40*, 213–226.
- (71) Von Der Esch, E.; Kohles, A. J.; Anger, P. M.; Hoppe, R.; Niessner, R.; Elsner, M.; Ivleva, N. P. TUM-ParticleType: A Detection and Quantification Tool for Automated Analysis of (Microplastic) Particles and Fibers. *PLoS One* **2020**, *15* (6 June), e0234766 DOI: [10.1371/journal.pone.0234766](https://doi.org/10.1371/journal.pone.0234766).
- (72) Su, L.; Sharp, S. M.; Pettigrove, V. J.; Craig, N. J.; Nan, B.; Du, F.; Shi, H. Superimposed Microplastic Pollution in a Coastal Metropolis. *Water Res.* **2020**, *168*, 115140.
- (73) Rolf, M.; Laermanns, H.; Kienzler, L.; Pohl, C.; Möller, J. N.; Laforsch, C.; Löder, M. G. J.; Bogner, C. Flooding Frequency and Floodplain Topography Determine Abundance of Microplastics in an Alluvial Rhine Soil. *Sci. Total Environ.* **2022**, 836 (December 2021), 155141 DOI: [10.1016/j.scitotenv.2022.155141](https://doi.org/10.1016/j.scitotenv.2022.155141).
- (74) Lusher, A. L.; Bråte, I. L. N.; Munno, K.; Hurley, R. R.; Welden, N. A. Is It or Isn’t It: The Importance of Visual Classification in Microplastic Characterization. *Appl. Spectrosc.* **2020**, *74* (9), 1139–1153.
- (75) Levi, D. M.; Klein, S. A. Seeing Circles: What Limits Shape Perception? *Vision Res.* **2000**, *40* (17), 97–107.
- (76) Napper, I. E.; Bakir, A.; Rowland, S. J.; Thompson, R. C. Characterisation, Quantity and Sorptive Properties of Microplastics Extracted from Cosmetics. *Mar. Pollut. Bull.* **2015**, *99* (1–2), 178–185.
- (77) Gewert, B.; Plassmann, M. M.; Macleod, M. Pathways for Degradation of Plastic Polymers Floating in the Marine Environment. *Environ. Sci.: Processes Impacts* **2015**, *17*, 1513–1521.
- (78) Duis, K.; Coors, A. Microplastics in the Aquatic and Terrestrial Environment: Sources (with a Specific Focus on Personal Care Products), Fate and Effects. *Environ. Sci. Eur.* **2016**, *28* (2), 2 DOI: [10.1186/s12302-015-0069-y](https://doi.org/10.1186/s12302-015-0069-y).
- (79) Lusher, A. L.; Hurley, R.; Arp, H. P. H.; Booth, A. M.; Bråte, I. L. N.; Gabrielsen, G. W.; Gomiero, A.; Gomes, T.; Grøsvik, B. E.; Green, N.; Haave, M.; Hallanger, I. G.; Halsband, C.; Herzke, D.; Jøner, E. J.; Kögel, T.; Rakkestad, K.; Rannekleiv, S. B.; Wagner, M.; Olsen, M. Moving Forward in Microplastic Research: A Norwegian

Perspective. *Environ. Int.* **2021**, *157* (August), 106794 DOI: 10.1016/j.envint.2021.106794.

(80) Perez, C. N.; Carré, F.; Hoarau-Belkhir, A.; Joris, A.; Leonards, P. E. G.; Lamoree, M. H. Innovations in Analytical Methods to Assess the Occurrence of Microplastics in Soil. *J. Environ. Chem. Eng.* **2022**, *10* (3), No. 107421.

(81) Fan, Y.; Zheng, J.; Deng, L.; Rao, W.; Zhang, Q.; Liu, T.; Qian, X. Spatiotemporal Dynamics of Microplastics in an Urban River Network Area. *Water Res.* **2022**, *212* (June 2021), No. 118116.

(82) Neelavannan, K.; Sen, I. S.; Lone, A. M.; Gopinath, K. Microplastics in the High-Altitude Himalayas: Assessment of Microplastic Contamination in Freshwater Lake Sediments, North-west Himalaya (India). *Chemosphere* **2022**, *290*. 133354.

(83) Gedik, K.; Eryaşar, A. R.; Gözler, A. M. The Microplastic Pattern of Wild-Caught Mediterranean Mussels from the Marmara Sea. *Mar. Pollut. Bull.* **2022**, *175*. 113331.

(84) Nizamali, J.; Mintenig, S. M.; Koelmans, A. A. Assessing Microplastic Characteristics in Bottled Drinking Water and Air Deposition Samples Using Laser Direct Infrared Imaging. *J. Hazard Mater.* **2023**, *441* (June 2022), No. 129942.

(85) Kooi, M.; Pimpke, S.; Mintenig, S. M.; Lorenz, C.; Gerdt, G.; Koelmans, A. A. Characterizing the Multidimensionality of Microplastics across Environmental Compartments. *Water Res.* **2021**, *202* (July), No. 117429.

(86) Simon-Sánchez, L.; Grelaud, M.; Lorenz, C.; Garcia-Orellana, J.; Vianello, A.; Liu, F.; Vollertsen, J.; Ziveri, P. Can a Sediment Core Reveal the Plastic Age? Microplastic Preservation in a Coastal Sedimentary Record. *Environ. Sci. Technol.* **2022**, *56* (23), 16780–16788.

(87) Bergmann, M.; Mützel, S.; Pimpke, S.; Tekman, M. B.; Trachsel, J.; Gerdt, G. White and Wonderful? Microplastics Prevail in Snow from the Alps to the Arctic. *Sci. Adv.* **2019**, *5* (8), No. eaax1157.

(88) Kooi, M.; Pimpke, S.; Mintenig, S. M.; Lorenz, C.; Gerdt, G.; Koelmans, A. A. Characterizing the Multidimensionality of Microplastics across Environmental Compartments. *Water Res.* **2021**, *202*. 117429.

(89) Zhao, G.; Mark, O.; Balstrøm, T.; Jensen, M. B. A Sink Screening Approach for 1D Surface Network Simplification in Urban Flood Modelling. *Water* **2022**, *14* (6), 963.

Recommended by ACS

Improved Reliability of Raman Spectroscopic Imaging of Low-Micrometer Microplastic Mixtures in Lake Water by Fractionated Membrane Filtration

Ziyan Wu, Haoran Wei, *et al.*

JUNE 12, 2023
ACS ES&T WATER

READ 

Machine Learning Prediction of Adsorption Behavior of Xenobiotics on Microplastics under Different Environmental Conditions

Michael Taylor Bryant and Xingmao Ma

JUNE 26, 2023
ACS ES&T WATER

READ 

Microplastics and Tire Wear Particles in Urban Stormwater: Abundance, Characteristics, and Potential Mitigation Strategies

Shima Ziajahromi, Frederic D. L. Leusch, *et al.*

AUGUST 14, 2023
ENVIRONMENTAL SCIENCE & TECHNOLOGY

READ 

High-Content Screening Discovers Microplastics Released by Contact Lenses under Sunlight

Yuxuan Liu, Bing Wu, *et al.*

JUNE 02, 2023
ENVIRONMENTAL SCIENCE & TECHNOLOGY

READ 

Get More Suggestions >